Hindawi
Advances in Civil Engineering
Volume 2023, Article ID 8853093, 12 pages
https://doi.org/10.1155/2023/8853093

Research Article

Analytical Study on Limiting Value of Shape Factor of Vertically Loaded Anchors in Saturated Soft Clay

Guoqi Xing,[1] **Yupeng Cao**,[1] **Baoliang Zhang**,[2] **Jian Li**,[2] **and Dapeng Li**[2]

[1]*School of Civil and Architectural Engineering, Weifang University, Weifang, Shandong, China*
[2]*School of Civil and Architectural Engineering, Liaocheng University, Liaocheng, Shandong, China*

Correspondence should be addressed to Guoqi Xing; xgq1105@163.com

Received 27 April 2023; Revised 29 June 2023; Accepted 9 August 2023; Published 25 August 2023

Academic Editor: Iman Mansouri

Copyright © 2023 Guoqi Xing et al. This is an open access article distributed under the Creative Commons Attribution License, which permits unrestricted use, distribution, and reproduction in any medium, provided the original work is properly cited.

The limiting values of shape factors are an important parameter for vertically loaded anchors (VLAs) at the deep-embedded depth, which influence the ultimate embedded depth and the maximum load-bearing capacity. The limiting values of load-bearing coefficients of VLAs which have different aspect ratios and different areas of fluke are obtained using the finite-element method. Furthermore, based on the expression of shape factors, the limiting values of shape factors of VLAs with different aspect ratios and different areas of a fluke are calculated. The influence of the aspect ratios and areas of fluke of VLAs on the shape factors is investigated. In addition, the effect of the shape factors of VLAs on the ultimate embedded depth and the maximum load-bearing capacity at the ultimate embedded depth is also studied. The results show that when the area of a fluke of VLAs is the same, decreasing the aspect ratio of a fluke can decrease the limiting value of shape factors; when the length of the fluke is constant, the area of the fluke has little influence on the limiting values of shape factors of VLAs. When the area of the fluke of VLAs is the same, the normalized ultimate embedded depth increases almost linearly with increasing the limiting value of shape factors and the maximum load-bearing capacity increases with increasing the limiting value of shape factors. The results can contribute to the design of the shape of a fluke of VLAs in soft clay.

1. Introduction

Drag anchors can be used as foundations in the mooring system [1], as shown in Figure 1. In general, the size and the shape of drag anchors influence the loading capacity and the capacity to penetrate into the soil, respectively [2]. It is very important to fully understand the loading capacity of drag anchors; therefore, some scholars have conducted the research on the loading capacity, such as O'Neill et al. [3], Merifield et al. [4], Merifield and Sloan [5], Song et al. [6], Aubeny and Chi [7], Tian et al. [8], Han et al. [9], Cheng et al. [10], Peccin da Silva et al. [11], and so on. The results obtained from the research on loading capacity of drag anchors show that, at the same embedded depth, the bigger the fluke of the drag anchor is, the larger the maximum load-bearing capacity; when the drag anchors have the same size of fluke, the deeper the drag anchor embeds into the soil, the larger the maximum load-bearing capacity is.

The reasonable shape of drag anchors can facilitate the penetration into the soil deeper and therefore it has a great influence on the embedded depth [12–14]. The development of the shape of drag anchors experiences three stages [15]. In the first stage, Stevin anchors, as shown in Figure 2(a), were used in the mooring system; however, because the shape of Stevin anchors was not conducive to penetrating into the soil [16], therefore they are not used in the mooring system up to now. In the second stage, Stevin anchors were replaced by Stevpris anchors shown in Figure 2(b), which can penetrate into the soil deeper compared to Stevin anchors; therefore, with the same bearing area of fluke, the maximum load-bearing capacity of Stevpris anchors is greater than Stevin anchors [15]. In the third stage, Stevmanta anchors, as shown in Figure 2(c), that is, vertically loaded anchors (VLAs), were extensively applied to mooring systems, attributing to lower cost, reusability, and high-bearing capacity; VLAs can withstand not only horizontal load but also vertical load [17]; therefore. it is widely applicable to the taut

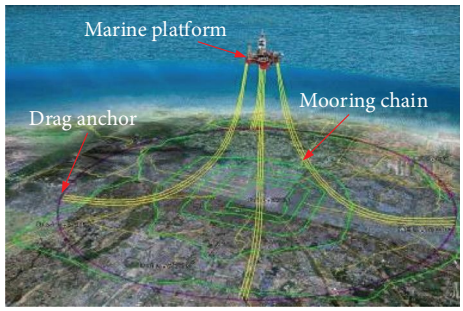

Figure 1: Mooring systems used in the marine platform.

mooring system in the deep sea [7]. In this paper, we only discuss the Stevmanta anchors, that is, the VLAs.

For the VLAs, it is essentially a plate [18]. To reveal the influence of the shape of the VLAs, that is, aspect ratio, on the maximum load-bearing capacity, Das et al. [19] has put forward the shape factor of the VLAs, which can be expressed as

$$f = \frac{N_c}{N_c^*}, \tag{1}$$

where N_c represents the load-bearing coefficient of VLAs with an aspect ratio not equal to 1.0; N_c^* represents the reference load-bearing coefficient of VLAs with an aspect ratio equal to 1.0, that is, square plate anchor. As can be noted from Equation (1) that the shape factor, f, actually represents the ratio of the maximum load-bearing capacity of the plate anchor with an aspect ratio not equal to 1.0 to the maximum load-bearing capacity of plate anchor with an aspect ratio equal to 1.0, which actually represents the change of bearing capacity of anchors.

On the basis of the concept of the shape factor, Das et al. [19] have carried out experiments with scaled models to investigate the shape factors of anchors. The results indicated that for the scaled models, the shape factors increased with increasing the embedment ratio; in addition, when the embedment ratio was the same, the aspect ratio of scaled models also influenced the shape factors. However, the limit values of shape factors for plate anchors, which have different aspect ratios are not investigated in experiments with scaled models.

In Det Norske Veritas (DNV) [20], for the plate anchor with an aspect ratio equal to 0.5, the shape factor f is considered as 1.1; in addition, the shape factor also reflects the transition from the strip anchor to the rectangular anchor under the plain strain condition. However, the shape factor in DNV [20] does not consider the embedded depth, and therefore, we cannot conclude whether the shape factor is a limiting value for plate anchors.

Based on the three-dimensional numerical modeling, Liu et al. [21] also investigated the shape factor of horizontally and vertically attached anchors and horizontally and vertically vented anchors. The results showed that the shape factor was related to the aspect ratio and embedded depth of plate anchors. However, the limit value of the shape factors for plate anchors which have different aspect ratios and different embedded depths at the deep-embedded depth in clay are not investigated.

Except that the shape factor can be obtained from the method defined above, the shape factor can be obtained through complex model tests [22]; however, some studies [1, 23] showed significant deviations from measured values, which indicate that it still remains difficulties to obtain the accurate shape factor by complex model tests.

Das et al. [19] considered that the maximum load-bearing capacity of plate anchors was related to the shape factor; therefore, the expression of the maximum load-bearing capacity of plate anchors was proposed as

$$P_u = f.\, N_c.\, A.\, S_u, \tag{2}$$

where P_u represents the maximum load-bearing capacity of the plate anchor; A is the effective area of the plate anchors; S_u is the undrained shear strength of the soil at the embedded anchor. As can be seen from Equation (2), the shape factor f has a significant influence on the maximum load-bearing capacity.

According to the theoretical analysis methods, the expression of the ultimate embedded depth of the drag anchor was derived by Neubecker and Randolph [24], Neubecker and Randolph [25]) as

$$Z_{\mathrm{UED}} = \frac{(\xi + 1).f.\, A_p.\, \theta_w}{2.b.\cos\theta_w}\left(\theta_w + \frac{2}{\eta_w}\right), \tag{3}$$

where b is the effective width of the embedded dragline; θ_w is the drag angle to the fluke at the shackle of the weightless anchor; A_p is the projected anchor area (in the direction of travel); and $\eta_w = T_w/W$ is the efficiency factor, where W is the submerged anchor weight and T_w is the drag force at the shackle of the weightless anchor; and ξ is the exponent. As illustrated in Equation (3), the shape factors also have a notable influence on the ultimate embedded depth of drag anchors. However, the influence of shape factors of plate anchors on the ultimate embedded depth of drag anchors has not been investigated up to now.

In this paper, the limiting values of the shape factor of plate anchors which have different aspect ratios and different areas of fluke at the deep-embedded depth in clay are obtained and the influence of the aspect ratios and the area of plate anchor on the limiting values of the shape factor of plate anchors at the deep-embedded depth is also investigated; in addition, the limiting values of shape factors of plate anchors are applied to investigating the influence on the maximum load-bearing capacity and the ultimate embedded depth at the deep-embedded depth.

2. Shape Factors of VLs in Clay at the Deep-Embedded Depth

Mackenzie [26] proposed the expression of the load-bearing coefficient of VLAs as

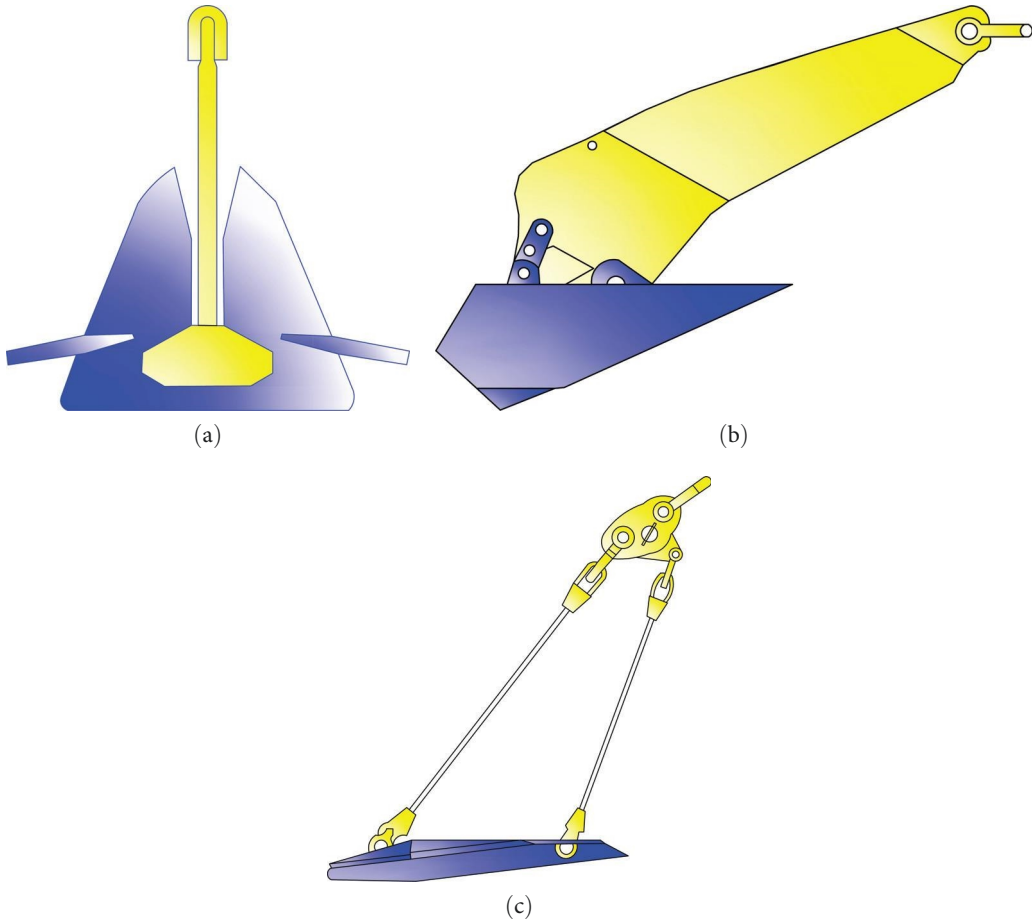

FIGURE 2: Drag anchors used in mooring system: (a) stevin; (b) stevpris; and (c) stevmanta anchors.

$$N_c = \frac{P_u}{A.\,S_u}, \tag{4}$$

where P_u is the maximum load-bearing capacity of anchors; A is the area of the anchor; and S_u is the undrained shear strength of clay. As can be seen from Equation (4), N_c increases with increasing the maximum load-bearing capacity of VLAs, P_u; however, the maximum load-bearing capacity is not always increasing with the embedded depth of VLAs when it is at the deep-embedded condition [27]. Therefore, there is a limiting value of the load-bearing coefficient for VLs. In this paper, we only investigate the limiting value of the load-bearing coefficient of VLAs at the deep-embedded depth. Furthermore, based on the equation for the shape factor as shown in Equation (1), the shape factor of VLAs can be obtained. Because N_c and N_c^* in Equation (1) are limiting values of the load-bearing coefficient; therefore, the shape factor obtained from Equation (1) is called the limiting value of shape factors of VLAs in this paper.

In this section, the numerical analysis is carried out using Z_SOIL [28] to determine the load-bearing coefficient of VLAs in clay.

To determine more accurately the maximum load-bearing capacity of VLAs, three-dimensional numerical modeling along with meshes is built, as indicated in Figure 3. To avoid the boundary effects in the finite-element model, the calculation range for soil should be large enough. Merifield and Sloan [4] considered that in the plane strain condition, the length and width of the calculation range for soil should be within about 16.0 B and the depth of the calculation range for soil should be not less than 5.0 B, where B was the length of the fluke of VLAs. In the three-dimensional numerical modeling as illustrated in Figure 3, the calculation range for soil in length and width direction are all set 21.0 B, and the distance from the VLA to the bottom of the calculation range is set 8.0 B. Moreover, considering the high plastic strain of soil near the VLAs, the dimensions of meshes for the soil near the VLAs are smaller compared with other regions, as shown in Figure 3. For soil and VLAs, eight-node continuum brick elements are used in the three-dimensional numerical modeling.

In addition, in Figure 3, the horizontal displacements at the lateral boundary of the calculation range for soil are constrained and the displacements at the bottom boundary in the x, y, and z directions are all constrained. However, the boundary at the top of the calculation range for soil is not constrained, which is in accordance with the actual stress of the pullout process. In addition, the load is applied to the centroid of the fluke of VLAs and it is perpendicular to the surface of the fluke, as indicated in Figure 3.

2.1. Constitutive Model and Parameters. The elastic-perfectly plastic model obeying Von Mises' yield criterion is often

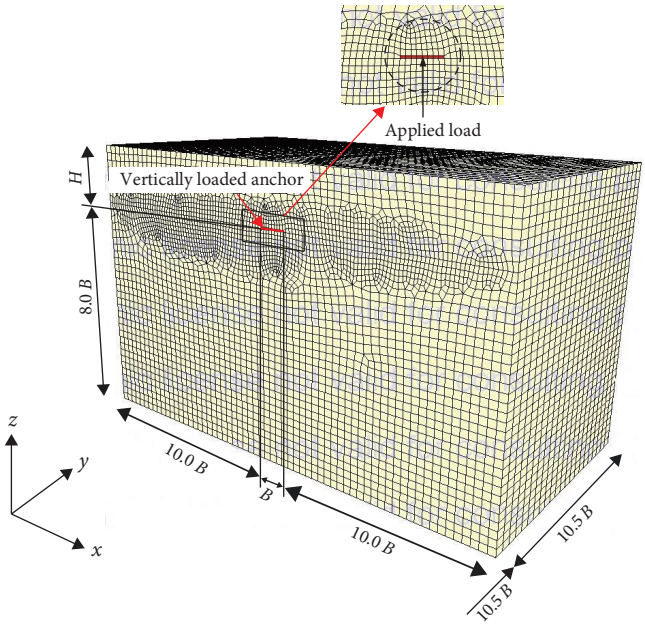

Figure 3: Finite-element model along with meshes.

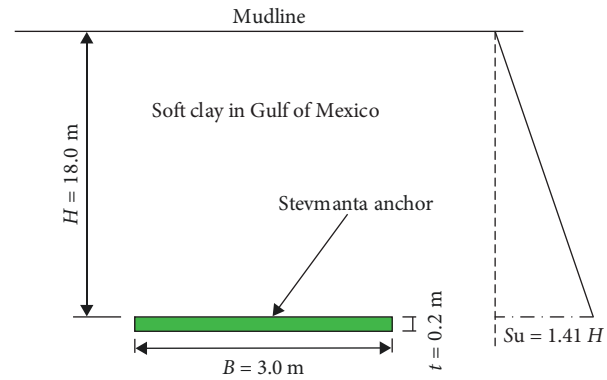

Figure 4: Schematic of field tests.

applied to clay [29]. The mechanical parameters for clay in the three-dimensional finite model are from the soft clay of the Gulf of Mexico [35]. The untrained shear strength of soft clay is $S_u = 1.41H$, where H is the embedded depth below the seabed in meters, as shown in Figure 3. The elastic modulus of clay E is $E = 1{,}000S_u$, and the Poisson's ratio of clay is $\nu = 0.49$. In addition, the yield stresses for soft clay is $\sqrt{3}S_u$ and the submerged unit weight of clay is 6.3 kN/m^3.

For the VLAs used in the field tests carried out by Ruinen [30], the linear elastic constitutive model is applied to them in the three-dimensional numerical modeling. The modulus of elasticity E and Poisson's ratio ν of VLAs are 2.06 GPa and 0.3, respectively. In addition, the submerged unit weight of the anchor is 68.0 kN/m^3.

In the three-dimensional numerical modeling, the surface of the VLAs is assumed smooth, that is, the friction between soil and anchor is not considered. In addition, in the pullout process of the VLAs, it is assumed that there is no suction force at the anchor base, that is, the vented anchors. In addition, considering that the coefficient of the lateral earth pressure K_0 is in the range of 0.8–1.85 [31]; therefore, the coefficient of the lateral earth pressure in numerical simulation calculations is assumed $K_0 = 1.0$ to obtain the initial geostatic stress for the three-dimensional numerical modeling.

In the numerical calculations, the first step is to determine the initial stress state with the coefficient of the lateral earth pressure K_0, which accounts for the effects of VLAs and clay. The second step is to exert the vertical load to the surface of the anchor fluke to obtain the maximum load-bearing capacity.

2.2. Validation of Finite-Element Model. To validate the credibility of the parameters of clay and VLAs as well as the meshes in the three-dimensional numerical modeling, the maximum load-bearing capacity of VLAs obtained from the three-dimensional numerical modeling should be compared with that from the field tests.

In the Gulf of Mexico, Ruinen [30] carried out field tests to determine the maximum load-bearing capacity of VLAs. In field tests, the VLAs were the Stevmanta anchors. The simplified dimension of the Stevmanta anchors was that the length and thickness of the anchor are 3.0 and 0.2 m, respectively, as shown in Figure 4; the width of the simplified dimension of the Stevmanta anchors is 1.0 and 3.0 m, respectively. The embedded depth of the anchors is 18.0 m. In addition, the undrained shear strength of soft clay of the Gulf of Mexico is represented as $S_u = 1.41H$. The mechanical parameters of the soft clay of the Gulf of Mexico and the Stevmanta anchor are the same as that in Section 2.1.

In field tests, the maximum load-bearing capacity of the Stevmanta anchor with the width of 1.0 and 3.0 m are 913.7 and 2741.1 kN, respectively.

Based on the three-dimensional numerical modeling as shown in Figure 3 and the mechanical parameters of soft clay of the Gulf of Mexico and the Stevmanta anchor in field tests, the displacement–load curve of the Stevmanta anchor can be determined, as shown in Figures 5(a) and 5(b). It is indicated from Figures 5(a) and 5(b) that, the maximum load-bearing capacity of the Stevmanta anchor with the width of 1.0 and 3.0 m are 896.1 and 2705.0 kN, respectively.

Compared with the results from the field tests, the error of the maximum load-bearing capacity of the Stevmanta anchor obtained from the three-dimensional numerical modeling is very small and the maximum error is only 1.93%. Therefore, the results obtained from the three-dimensional numerical modeling are credible.

2.3. Influence of Aspect Ratio of a VLA in Clay on the Limiting Value of Shape Factors. A VLA essentially is a plate anchor, thus it is important to discuss the influence of the aspect ratio and area of the VLAs on the limiting value of shape factors. To obtain the limiting value of shape factors of a VLA in clay, the limiting value of load-bearing coefficients should be first obtained. In this section, the area of VLAs is set 4.0, 9.0, 16.0, and 25.0 m^2, which are the commonly used area of VLAs [32]. When the area of the VLAs is equal, changing the aspect ratio of the VLAs in clay can investigate the influence of the aspect ratio on the shape factor. When the area of

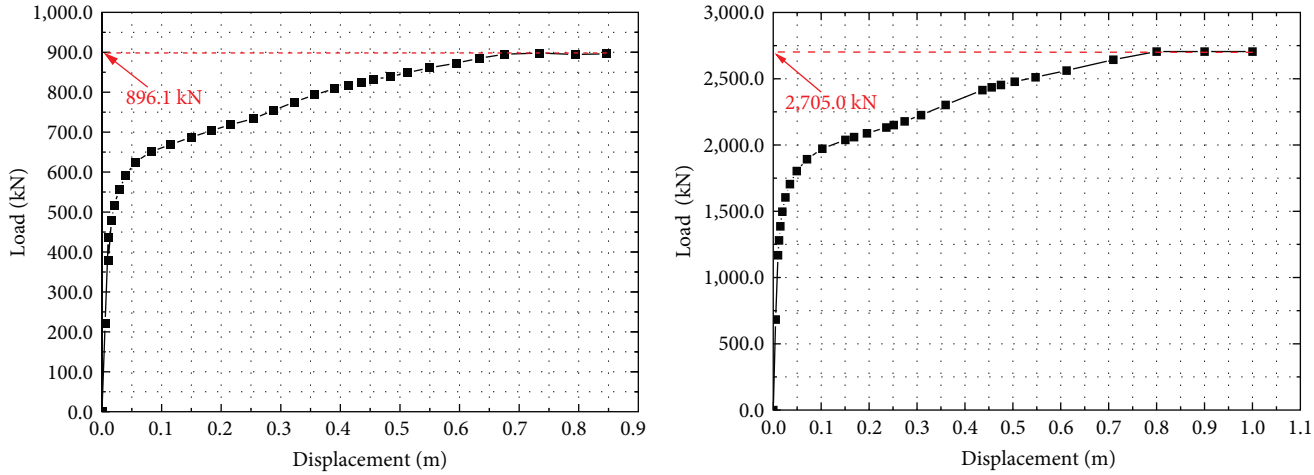

FIGURE 5: The curve of load versus displacement from the finite-element method. (a) Width = 1.0 m, and (b) width = 3.0 m.

VLAs is 4.0 m^2, the lengths of VLAs are set 4.0, 3.5, 3.0, 2.5, and 2.0 m; therefore, the aspect ratios of VLAs are 4 : 1, 49 : 16, 9 : 4, 25 : 16, and 1 : 1. When the area of the VLAs is 9.0 m^2, the lengths of VLAs are set to 6.0, 5.0, 4.5, 4.0, and 3.0 m; therefore, the aspect ratios of VLAs are 4 : 1, 25 : 9, 9 : 4, 16 : 9, and 1 : 1. When the area of VLAs is 16.0 m^2, the lengths of VLAs are 6.0, 5.5, 5.0, 4.5, and 4.0 m; therefore, the aspect ratios of VLAs are 9 : 4, 121 : 64, 25 : 16, 81 : 64, and 1 : 1. When the area of VLAs is 25.0 m^2, the lengths of VLAs are set to 8.0, 7.5, 7.0, 6.5, 6.0, 5.5, and 5.0 m; therefore, the aspect ratios of VLAs are 64 : 25, 9 : 4, 49 : 25, 169 : 100, 36 : 25, 121 : 100, and 1 : 1. In addition, the thickness of VLAs in the three-dimensional numerical modeling is all set 0.2 mm. For VLAs, the critical embedded depth is about 3.0–4.5 times the length of the fluke in clay [20, 33]. In the three-dimensional numerical modeling, the embedded depth of VLAs H, as shown in Figure 3, is all set 5.0B (B represents the length of the fluke), which is greater than the critical embedded depth (4.5B). Therefore, all the anchors studied in this paper are deep-embedded VLAs and the limiting value of the load-bearing coefficients of VLAs can be obtained.

Based on the numerical analysis method, the maximum load-bearing capacity of VLAs at the deep-embedded depth can be obtained. The load-bearing coefficient N_c of VLAs with different aspect ratios in clay, can be further calculated with Equation (4), the calculation results are indicated in the Figure 6(a)–6(d). As can be seen from Figure 6(a)–6(d), when the area of the fluke of VLAs is the same, the limiting value of load-bearing coefficients all decreases with increasing the length of the fluke, that is, the limiting value of load-bearing coefficients decreases with decreasing the aspect ratio of VLAs. In addition, Figure 6(a)–6(d) also shows that the VLAs with an aspect ratio equal to 1.0, that is, square anchor, have the maximum load-bearing coefficients compared with that with other aspect ratios.

The limiting value of shape factors of VLAs with different aspect ratios can be further calculated with Equation (1). Liu et al. [22] considered that when the area of the drag anchor is larger, it cannot conveniently penetrate into the seabed; therefore, the area of the drag anchor should not be too large. Gourvenec and Cassidy [32] considered that the maximum area of VLAs should not be greater than 25.0 m^2. In this section, the reference load-bearing coefficient N_c^* in Equation (1) is selected as 7.816, which corresponds to the limiting value of the load-bearing coefficient of VLAs with an aspect ratio of 1.0 and an area of 25.0 m^2. Figure 7 shows the influence of the length of the fluke on the limiting value of the shape factor of VLAs which have different areas of the fluke. It is indicated from Figure 7 that, when the area of fluke of VLAs is the same, increasing the length of the fluke (i.e., decreasing the aspect ratio) can reduce the limiting value of shape factors of VLAs. In addition, as illustrated in Figure 7, when the length of the fluke of VLAs is 5.0 m, all the limiting values of shape factors of anchors with different areas of the fluke are equal to 1.0; when the length of the fluke of VLAs is 4.0 m, all the limiting values of shape factors of anchors with different areas of the fluke are greater than 1.0; however, when the length of the fluke of VLAs is 6.0 m, all the limiting values of shape factors of anchors with different areas of the fluke are less than 1.0.

On the basis of the results from Figure 7, the influence of the area of the fluke of VLAs on the limiting value of shape factors can also be obtained. It is indicated from Figure 7, the variation of the area of the fluke of VLAs has little influence on the shape factors when the length of the fluke is the same. Figure 7 also shows that, when the length of the fluke is constant, the area of the fluke has almost no effect on the shape factor of VLAs.

3. Application of Shape Factor to VLAs at the Deep-Embedded Depth

3.1. Application of Shape Factors to Ultimate Embedded Depth. For soil with strength proportional to depth, that is, $S_u = k.z$, where k is the soil strength gradient, Neubecker and Randolph [25] considered that when the anchor was at the ultimate embedded depth, the efficiency of anchors η_w in Equation (3) can be expressed as

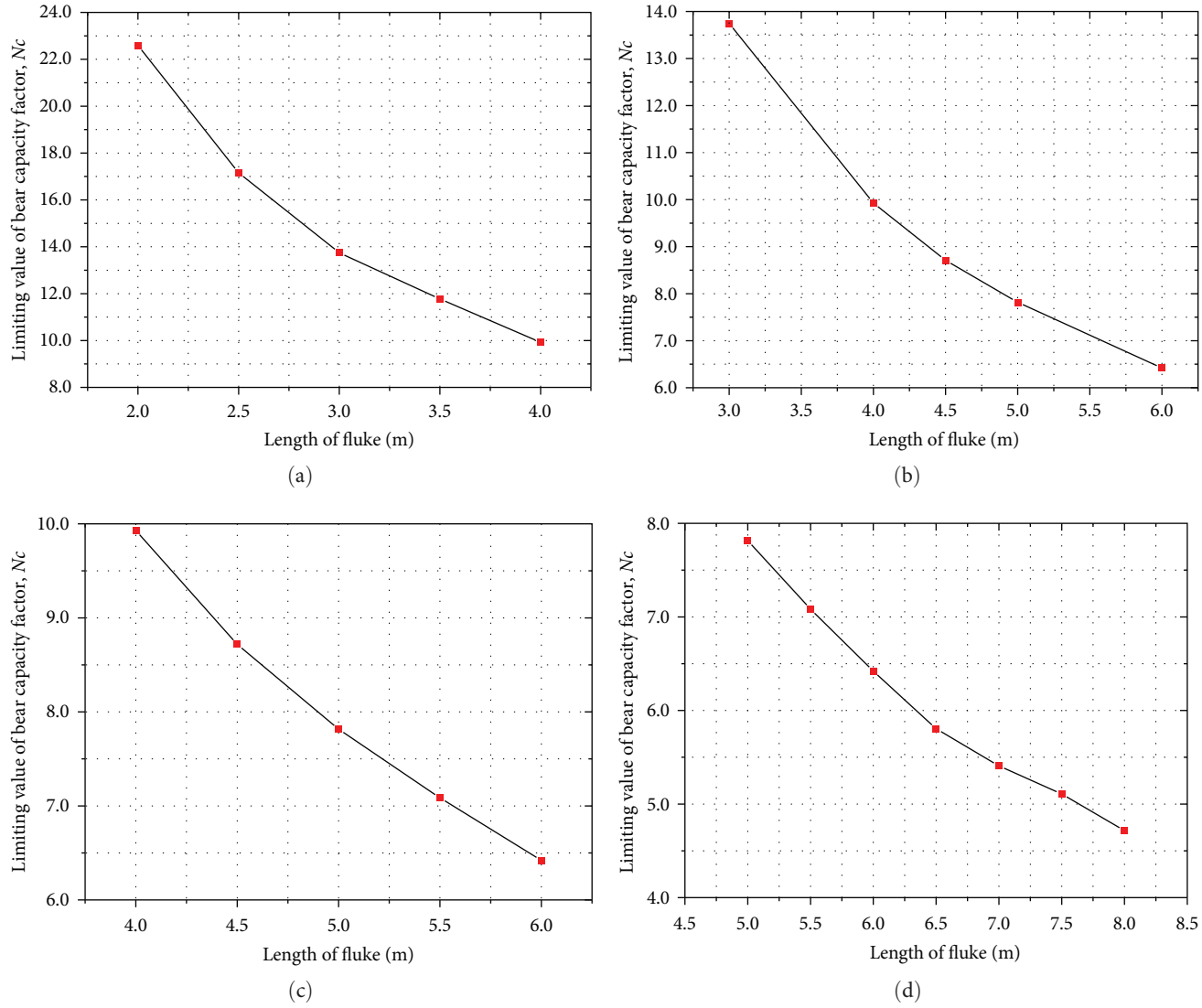

FIGURE 6: Variation of limiting value (VLA) of load-bearing coefficient with the length of a fluke. Area of fluke (a) 4.0, (b) 9.0, (c) 16.0, and (d) 25.0 m^2.

$$\eta_w = \frac{f.\,A_p.\,N_c.\,k.\,Z_{\mathrm{UED}}}{W.\cos\theta_w}. \tag{5}$$

Equation (5) is substituted into Equation (3) and (3) can be rewritten as

$$Z_{\mathrm{UED}} = \frac{(\xi+1).f.\,A_p.\,\theta_w}{2.\,b.\cos\theta_w}\left(\theta_w + \frac{2.\,W.\cos\theta_w}{f.\,A_p.\,N_c.\,k.\,Z_{\mathrm{UED}}}\right), \tag{6}$$

where $\xi = 1$ corresponds to the soil with strength proportional to depth.

Based on Equation (6), the ultimate embedded depth Z_{UED} for anchors in soil with strength proportional to depth can be calculated as

$$Z_{\mathrm{UED}} = \frac{n + \sqrt{n^2 + 4.\,m.\,p}}{2.\,m}, \tag{7}$$

where $m = b.\,N_c.\,k.\cos\theta_w$, $n = f.\,N_c.\,k.\,\theta_w.\,A_p$, $p = 2.\,W.\cos\theta_w$.

Dunnavant and Kwan [34] conducted some centrifuge tests on plate anchors and found that the anchor flukes were almost horizontal when they were at ultimate embedded depth. For VLAs with anchor bridles as shanks at the ultimate embedded depth, the drag angle to the fluke at the shackle of the anchors θ_w in Equation (7) is shown in Figure 8 and it is assumed to be 0.2 in this section. In Equation (7), the effective width of the bridle b is assumed to be 0.25 m; the density of anchors is 7,800 kg/m^3 and the soil strength gradient of soil k is assumed to be 1.41.

To investigate the influence of shape factors on the ultimate embedded depth of VLAs at the deep-embedded depth in clay with strength proportional to depth based on Equation (7), the length, width, and thickness of VLAs is selected and

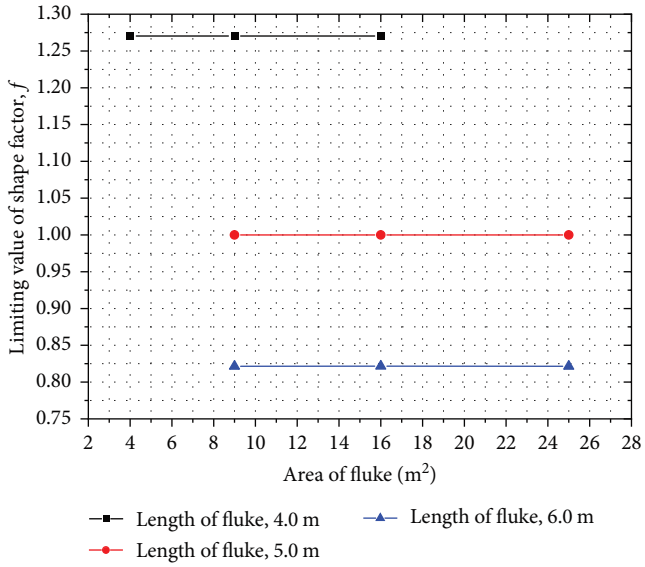

Figure 7: Variation of limiting value of shape factor with the area of the fluke.

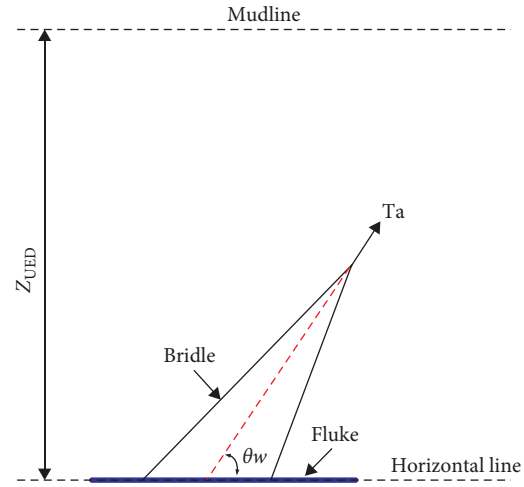

Figure 8: VLAs at ultimate embedded depth.

Table 1: Parameters used in Equation (7) for VLAs in clay with strength proportional to the depth.

Aspect ratio	Length and thickness of anchor (m)	Limiting value of shape factors, f	Projected area, A_p (m^2)	Submerged weight, W (kN)	Limiting value of load-bearing coefficients, N_c
1 : 1	2.0, 0.2	2.89	4.0	53.3	22.59
25 : 16	2.5, 0.2	2.20	4.0	53.3	17.16
9 : 4	3.0, 0.2	1.76	4.0	53.3	13.75
49 : 16	3.5, 0.2	1.51	4.0	53.3	11.77
4 : 1	4.0, 0.2	1.27	4.0	53.3	9.93
1 : 1	3.0, 0.2	1.76	9.0	120.0	13.75
16 : 9	4.0, 0.2	1.27	9.0	120.0	9.93
9 : 4	4.5, 0.2	1.11	9.0	120.0	8.71
25 : 9	5.0, 0.2	1.00	9.0	120.0	7.82
4 : 1	6.0, 0.2	0.82	9.0	120.0	6.42
1 : 1	4.0, 0.2	1.27	16.0	213.3	9.93
81 : 64	4.5, 0.2	1.12	16.0	213.3	8.72
25 : 16	5.0, 0.2	1.0	16.0	213.3	7.82
121 : 64	5.5, 0.2	0.91	16.0	213.3	7.09
9 : 4	6.0, 0.2	0.82	16.0	213.3	6.42
1 : 1	5.0, 0.2	1.00	25.0	333.3	7.82
121 : 100	5.5, 0.2	0.91	25.0	333.3	7.08
36 : 25	6.0, 0.2	0.82	25.0	333.3	6.42
169 : 100	6.5, 0.2	0.74	25.0	333.3	5.80
49 : 25	7.0, 0.2	0.69	25.0	333.3	5.41
9 : 4	7.5, 0.2	0.65	25.0	333.3	5.25
64 : 25	8.0, 0.2	0.60	25.0	333.3	5.01

are illustrated in Table 1. The other parameters in Equation (7) for VLAs are also shown in Table 1. The limiting values of load-bearing coefficients and the limiting values of shape factors in Table are from Figure 6(a)–6(d) and Figure 9(a)–9(d). According to Equation (7) and the parameters shown in Table 1, the influence of the limiting value of shape factors of VLAs on the normalized ultimate embedded depth can be obtained, as shown in Figure 10(a)–10(d).

As illustrated in Figure 10(a)–10(d), when the area of the fluke of VLAs is the same, the normalized ultimate embedded depth Z_{UED}/B increases almost linearly with increasing the limiting value of shape factors. In addition, it all indicates from Figure 10 that the VLAs with an aspect ratio equal to 1.0, that is, square anchor plates, penetrate into the soil deeper than rectangular anchor plates when the area of the fluke of VLAs is the same. For the rectangular anchors, as the area

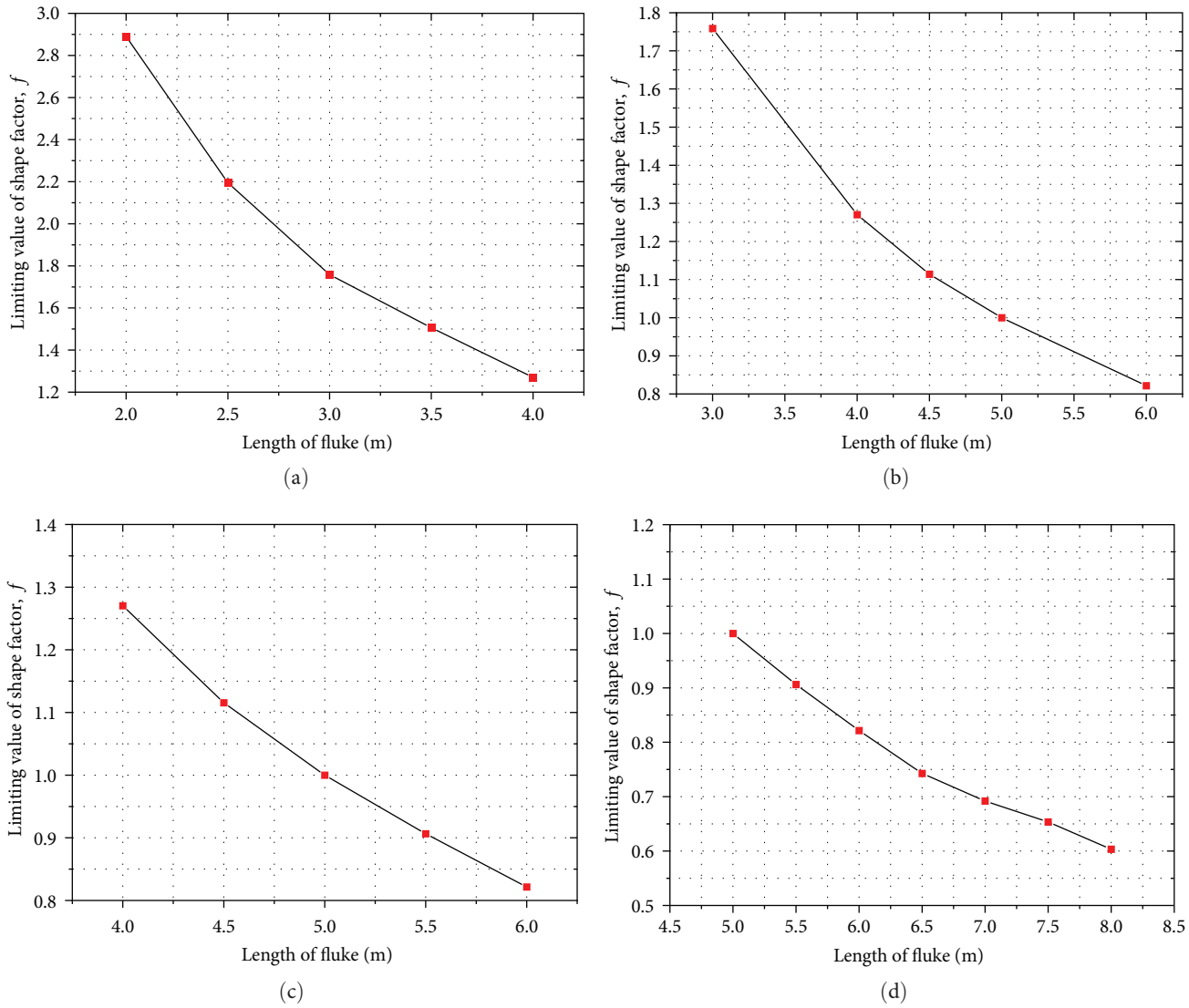

FIGURE 9: VLA of shape factor with the length of the fluke of VLAs. Area of fluke (a) 4.0, (b) 9.0, (c) 16.0, and (d) 25.0 m^2.

of the fluke of VLAs is the same, the larger the length of the fluke of VLAs is, the smaller the normalized ultimate embedded depth is. Figure 11 indicates the variation of the normalized ultimate embedded depth with the area of fluke of VLAs as the limiting values of shape factors of VLAs with different areas of the fluke are the same. It is indicated from Figure 11, when the limiting values of shape factors are the same for VLAs, the normalized ultimate embedded depth of VLAs increases with enlarging the area of the fluke; in addition, when the shape factor is not greater than 1.00, the normalized ultimate embedded depth of VLAs almost linearly increases with enlarging the area of the fluke.

3.2. Application of Shape Factors to Ultimate Pullout Capacity at the Ultimate Embedded Depth. To investigate the influence of shape factors on the maximum load-bearing capacity of VLAs based on Equation (2), the length, width, and thickness of VLAs are selected and they are the same as that in Table 1. In addition, the parameters used in Equation (2), such as shape factor f, effective area A, undrained shear strength S_u, and load-bearing coefficient N_c, for VLAs are the same as that in Table 1. In the three-dimensional numerical modeling, the undrained shear strengths of clay used in Equation (2) are also assumed as $S_u = 1.41.z$ and VLAs are also at the deep-embedded depth. Based on Equation (2), the maximum load-bearing capacity of VLAs with different shape factors can be obtained and furthermore, the influence of the shape factor on the maximum load-bearing capacity of VLAs is investigated, as illustrated in Figure 12.

As shown in Figure 12(a)–12(d), when the area of the fluke of VLAs is the same, the maximum load-bearing capacity of VLAs increases with increasing the shape factors. In addition, it also indicated in Figure 12 that when the area of the fluke of VLAs is the same, the maximum load-bearing capacity of VLAs with an aspect ratio of 1.0, that is, square anchor, is greater than that with an aspect ratio not equal to 1.0, that is, rectangular anchor. For the rectangular anchors, when the area of the fluke of VLAs is the same, the larger the

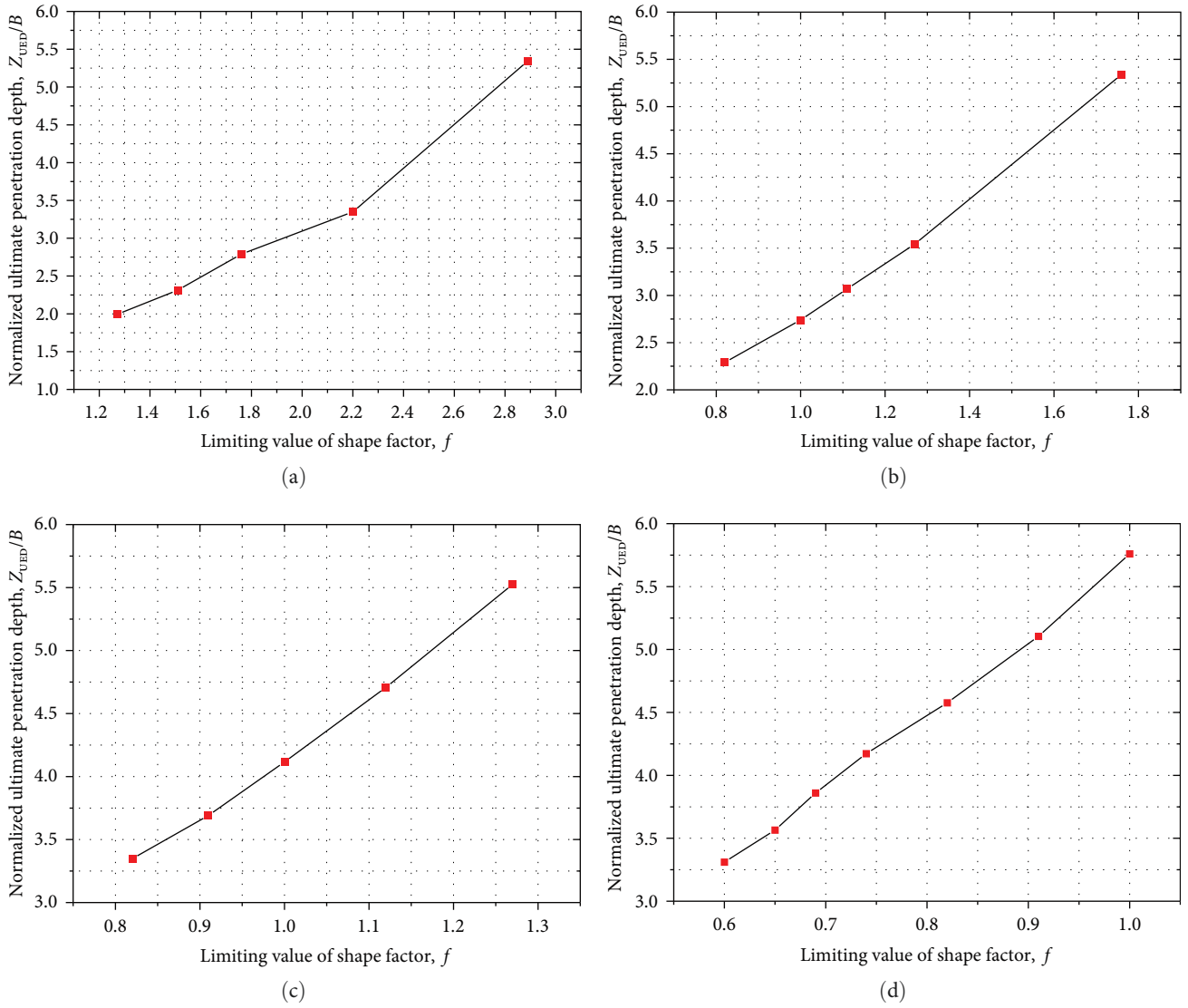

Figure 10: Variation of ultimate embedded depth with limiting values of shape factors of VLAs. Area of fluke (a) 4.0, (b) 9.0, (c) 16.0, and (d) 25.0 m^2.

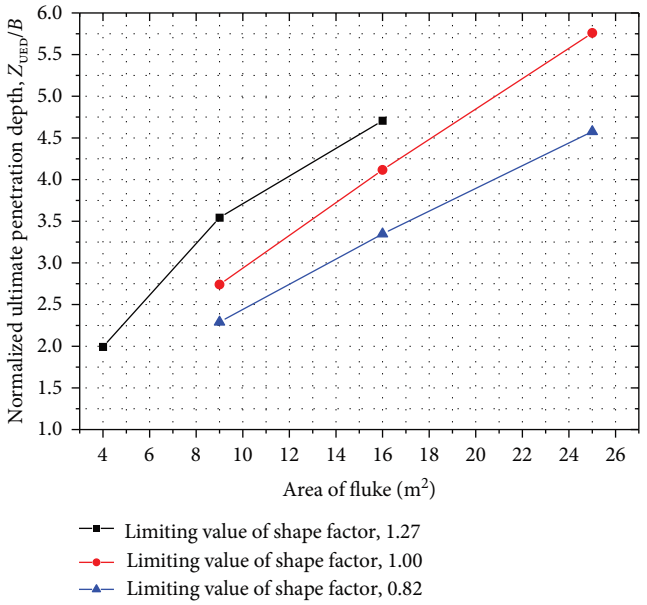

Figure 11: Variation of ultimate embedded depth with the area of the fluke of VLAs.

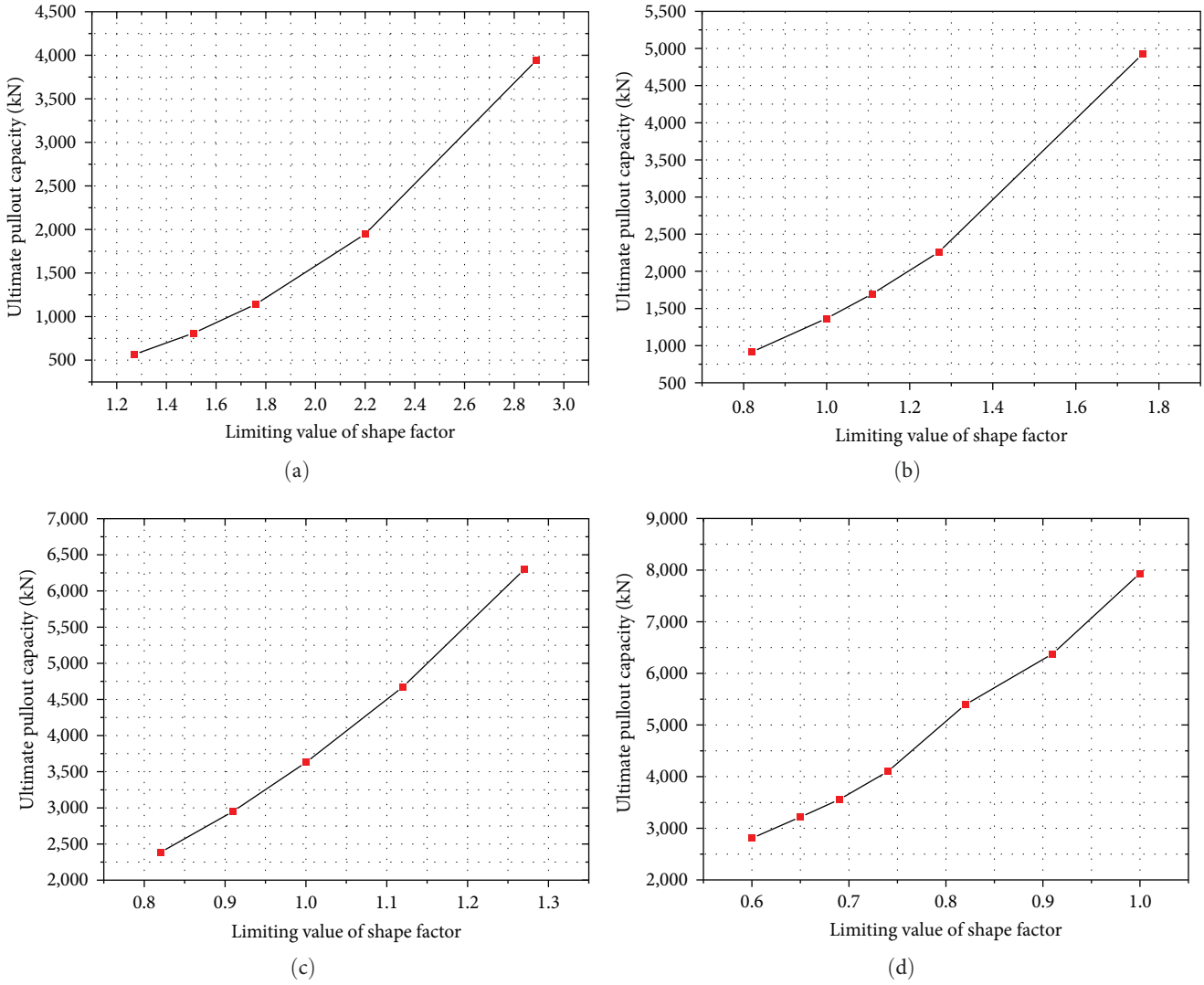

Figure 12: Variation of ultimate pullout capacity with shape factors of VLAs. Area of fluke (a) 4.0, (b) 9.0, (c) 16.0, and (d) 25.0 m^2.

length of the fluke of VLAs is, the smaller the maximum load-bearing capacity is. Figure 13 shows the variation of the maximum load-bearing capacity with the area of the fluke of VLAs as the shape factors remain constant. As can be seen from Figure 13, when the shape factors are the same for VLAs, the maximum load-bearing capacity of VLAs increases with enlarging the area of the fluke.

4. Conclusions

Based on the finite-element method, the limiting values of the maximum load-bearing capacity of VLAs in clay with strength proportional to the depth are obtained. Furthermore, according to the expression of load-bearing coefficients, the limiting values of load-bearing coefficients of VLAs are obtained. Moreover, based on the expression of the shape factors, the limiting values of the shape factors of VLAs with different areas of the fluke and different aspect ratios of the fluke are obtained. The influence of the area of the fluke and the aspect ratio of the fluke on the shape factors of VLAs are investigated. In addition, the effect of the shape factors of VLAs on the ultimate embedded depth and ultimate pullout capacity is also studied in this paper. The following results are drawn from the study.

(1) When the area of the fluke of VLAs is the same, the limiting value of load-bearing coefficients all decreases with increasing the length of the fluke, that is, the limiting value of load-bearing coefficients decreases with decreasing the aspect ratio of VLAs. The VLAs with an aspect ratio equal to 1.0, that is, square anchor, have the maximum load-bearing coefficients compared with that of other aspect ratios.

(2) When the area of the fluke of VLAs is the same, increasing the length of the fluke (i.e., decreasing the aspect ratio) can reduce the limiting value of shape factors of VLAs; when the length of the fluke is constant, the area of the fluke has little influence on the shape factor of VLAs.

(3) When the area of the fluke of VLAs is the same, the normalized ultimate embedded depth increases almost

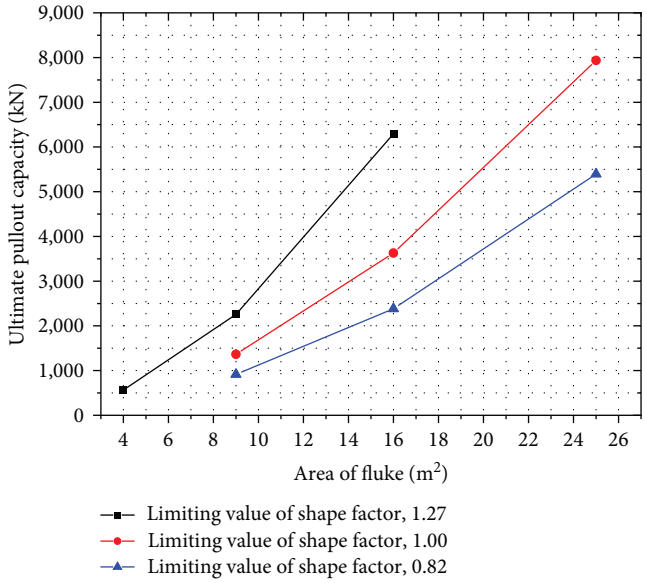

FIGURE 13: Variation of ultimate pullout capacity with the area of the fluke of VLAs.

linearly with increasing the limiting value of shape factors and the VLAs with aspect ratio equal to 1.0, that is, square anchor plates, penetrate into the soil deeper than rectangular anchor plate. For the rectangular anchors, as the area of the fluke of VLAs is the same, the larger the length of the fluke of VLAs is, the smaller the normalized ultimate embedded depth is. When the limiting values of shape factors are the same for VLAs, the normalized ultimate embedded depth of VLAs increases with enlarging the area of the fluke.

(4) When the area of the fluke of VLAs is the same, the maximum load-bearing capacity of VLAs with an aspect ratio of 1.0, that is, square anchor, is greater than that with an aspect ratio not equal to 1.0, that is, rectangular anchor. For the rectangular anchors, when the area of the fluke of VLAs is the same, the larger the length of fluke of VLAs is, the smaller the maximum load-bearing capacity is. When the shape factors are same for VLAs, the maximum load-bearing capacity of VLAs increases with enlarging the area of the fluke.

The above research results mainly contribute to the design of the VLAs in single clay with strength proportional to the depth. Reasonable shape factors, that is, smaller shape factors, and reasonable area of the fluke, that is, larger area of the fluke, can make the ultimate embedded depth of VLAs deeper and the maximum load-bearing capacity larger.

However, the above research results are only applicable to the vented VLAs, that is, not consider the influence of the suction force at the anchor base; in addition, the ultimate embedded depth of VLAs is suitable to the situation where the fluke of VLAs is in the horizontal when the VLAs do not continuously penetrate into clay. Moreover, further research should be conducted to investigate whether the above research results are applicable to layered soil.

Data Availability

The raw/processed data required to reproduce these findings cannot be shared at this time as the data also forms part of an ongoing study.

Conflicts of Interest

The authors declare that they have no financial or personal relationships with anyone or any entity whose interests could be positively or negatively influenced by the content of this paper.

Acknowledgments

The authors thank the peer reviewers and Editor for their valuable comments and suggestions, which have greatly improved the manuscript. In addition, the authors are also grateful to Mr. Wei Xuan, Ms. Rong Wang, and Ms. Xinghua Ju for their generous assistance with this work. This work was financially supported by the National Natural Science Foundation of China (Grant No. 52178347) and the Natural Science Foundation of Shandong Province (Grant Nos. ZR2022ME165 and ZR2021ME068).

References

[1] M. O'Neill and M. Randolph, "Modelling drag anchors in a drum centrifuge," *International Journal of Physical Modelling in Geotechnics*, vol. 1, no. 2, pp. 29–41, 2001.

[2] A. Aslkhalili, H. Shiri, and S. Zendehboudi, "Reliability assessment of drag embedment anchors in sand and the effect of idealized anchor geometry," *Safety in Extreme Environments*, vol. 2, pp. 37–55, 2020.

[3] M. P. O'Neill, M. F. Randolph, and A. R. House, "The behaviour of drag anchors in layered soils," *International Journal of Offshore and Polar Engineering*, vol. 9, no. 1, pp. 73–78, 1999.

[4] R. S. Merifield, S. W. Sloan, and H. S. Yu, "Stability of plate anchors in undrained clay," *Géotechnique*, vol. 51, no. 2, pp. 141–153, 2001.

[5] R. S. Merifield and S. W. Sloan, "The ultimate pullout capacity of anchors in frictional soils," *Canadian Geotechnical Journal*, vol. 43, no. 8, pp. 852–868, 2006.

[6] Z. H. Song, Y. X. Hu, and M. F. Randolph, "Numerical simulation of vertical pullout of plate anchors in clay," *Journal of Geotechnical and Geoenvironmental Engineering*, vol. 134, no. 6, pp. 866–875, 2008.

[7] C. Aubeny and C.-M. Chi, "Analytical model for vertically loaded anchor performance," *Journal of Geotechnical and Geoenvironmental Engineering*, vol. 140, no. 1, pp. 14–24, 2014.

[8] Y. Tian, M. F. Randolph, and M. J. Cassidy, "Analytical solution for ultimate embedment depth and potential holding capacity of plate anchors," *Géotechnique*, vol. 65, no. 6, pp. 517–530, 2015.

[9] C. Han, D. Wang, C. Gaudin, C. D. O'Loughlin, and M. J. Cassidy, "Behaviour of vertically loaded plate anchors

under sustained uplift," *Géotechnique*, vol. 66, no. 8, pp. 681–693, 2016.

[10] X. L. Cheng, Y. F. Li, P. G. Wang, Z. X. Liu, and Y. D. Zhou, "Model tests and finite element analysis for vertically loaded anchors subjected to cyclic loads in soft clays," *Computers and Geotechnics*, vol. 119, Article ID 103317, 2020.

[11] A. Peccin da Silva, A. Diambra, D. Karamitros, and S. H. Chow, "A non-associative macroelement model for vertical plate anchors in clay," *Canadian Geotechnical Journal*, vol. 58, no. 11, pp. 1703–1715, 2021.

[12] H. X. Liu, Y. Li, H. Yang, W. Zhang, and C. L. Liu, "Analytical study on the ultimate embedment depth of drag anchors," *Ocean Engineering*, vol. 37, no. 14–15, pp. 1292–1306, 2010.

[13] W. Zhang, X. Z. Li, and Q. P. Li, "Research on experiment and shape-optimization of drag anchors," *Ship Engineering*, vol. 35, no. 6, pp. 43–46, 2013.

[14] G. Q. Xing, Y. P. Cao, B. L. Zhang, J. Li, and X. T. Zhang, "Influence of parameters on the ultimate penetration depth of a double-plate vertically loaded anchor in soft clay," *Frontiers in Materials*, vol. 10, Article ID 1225258, 2023.

[15] V. Anchors, *Anchor Manual*, Krimpen ad Yssel, The Netherlands, 2005.

[16] R. K. Rowe and E. H. Davis, "The behaviour of anchor plates in clay," *Géotechnique*, vol. 32, no. 1, pp. 9–23, 1982.

[17] M. Yang, J. D. Murff, and C. P. Aubeny, "Undrained capacity of plate anchors under general loading," *Journal of Geotechnical and Geoenvironmental Engineering*, vol. 136, no. 10, pp. 1383–1393, 2010.

[18] D.-S. Qiao, B. Guan, H.-Z. Liang, D.-Z. Ning, B.-B. Li, and J.-P. Ou, "An improved method of predicting drag anchor trajectory based on the finite element analyses of holding capacity," *China Ocean Engineering*, vol. 34, pp. 1–9, 2020.

[19] B. M. Das, R. Moreno, and K. F. Dallo, "Ultimate pullout capacity of shallow vertical anchors in clay," *Soils and Foundations*, vol. 25, no. 2, pp. 148–152, 1985.

[20] Det Norske Veritas(DNV), *RP-E302 Design and Installation of Drag-in Plate Anchors in Clay*, Det Norske Veritas, Norwegian, 2002.

[21] J. Liu, M. Tan, and Y. Hu, "New analytical formulas to estimate the pullout capacity factor for rectangular plate anchors in NC clay," *Applied Ocean Research*, vol. 75, pp. 234–247, 2018.

[22] H. Liu, W. Zhang, X. Zhang, and C. Liu, "Experimental investigation on the penetration mechanism and kinematic behavior of drag anchors," *Applied Ocean Research*, vol. 32, no. 4, pp. 434–442, 2010.

[23] M. P. O'Neill, M. F. Randolph, and S. R. Neubecker, in *Paper presented at the The Seventh International Offshore and Polar Engineering Conference*, Honolulu, Hawaii, USA, May 1997.

[24] S. R. Neubecker and M. F. Randolph, "Profile and frictional capacity of embedded anchor chain," *Journal of Geotechnical Engineering*, vol. 121, no. 11, pp. 797–803, 1995.

[25] S. R. Neubecker and M. F. Randolph, "The performance of drag anchor and chain system in cohesive soil," *Marine Georesources & Geotechnology*, vol. 14, no. 2, pp. 77–96, 1996.

[26] T. R. Mackenzie, *Strength of deadman anchor in clay*, Princeton, NJ., USA, M.S. Thesis presented to Princeton University, 1955.

[27] Det Norshke Veritas (DNV), *Rp-e301 Design and Installation of Fluke Anchors in Clay*, Det Norske Veritas, Norwegian, 2000.

[28] Zace Services Ltd, *Zsoil.Pc2011 Manual*, Elmepress International, Lausanne, Switzerland, 2011.

[29] D. S. Qiao and J. P. Ou, "Analysis on ultimate pullout bearing capacity of drag embedment anchor under cyclic loading," *Journal of Harbin Institute of Technology*, vol. 44, no. 12, pp. 112–117, 2012.

[30] R. M. Ruinen, "Penetration analysis of drag embedment anchors in soft clays," in *Proceedings of the 14th International Offshore and Polar Engineering Conference*, pp. 531–537, ISOPE, Toulon, France, 2004.

[31] K. H. Andersen, H. P. Jostad, and R. Dyvik, "Penetration resistance of offshore skirted foundations and anchors in dense sand," *Journal of Geotechnical and Geoenvironmental Engineering*, vol. 134, no. 1, pp. 106–116, 2008.

[32] S. Gourvenec and M. Cassidy, "Vertically loaded plate anchors for deepwater applications," in *Frontiers in Offshore Geotechnics: Proceedings of the International Symposium on Frontiers in Offshore Geotechnics (IS-FOG 2005)*, pp. 31–48, CRC Press, The Netherlands, 2005.

[33] R. M. Ruinen and G. Degenkamp, "Anchor selection and installation for shallow and deepwater mooring systems," in *Proceedings of the 11th International Offshore and Polar Engineering Conference*, ISOPE, Stavanger, Norway, 2001.

[34] T. W. Dunnavant and C.-T. T. Kwan, "Centrifuge modeling and parametric analyses of drag anchor behavior," in *Proceedings of the 25th Annual Offshore Technology Conference*, OTC, Houston, Texas, 1993.

[35] B. Sukumaran, W. O. McCarron, P. Jeanjean, and H. Abouseeda, "Efficient finite element techniques for limit analysis of suction caissons under lateral loads," *Computers and Geotechnics*, vol. 24, no. 2, pp. 89–107, 1999.